

# Analysis and Improved Design of Gamma-Ray Backscattering Density Gages

K. PREISS, Assistant Professor of Civil and Nuclear Engineering, University of Illinois

The nuclear reactions which gamma radiation may undergo in a material of medium atomic weight, such as soil, are discussed and related to the properties of backscattering density gages. Theoretical reasoning and experimental evidence are presented to show that the effect of the chemical composition of the material may be eliminated when: (a) the detector "sees" material near the source, and (b) photons of energy below 0.1 mev are not detected. The latter may be achieved with a scintillation counter and pulse selector or by placing iron filters in front of a Geiger-Müller tube. The geometry defined by (a) causes the peak in the calibration curve to move to a density so high that the count rate becomes a unique measure of density, rising over the entire range of density from 0 to 160 pcf. Errors in the density reading due to the statistics of nuclear counting and surface roughness are discussed.

•INSTRUMENTS which measure the density of soils by gamma-ray backscatter have been in use for some years. There has been conflicting experimental evidence as to whether the type or chemistry of the soil tested affected the instrument reading. Neville and van Zelst (13), Gnaedinger (5), Mintzer (12), Kuhn (9), and others have found such an effect, but Carlton (3) and Huet (8) reported that, for the soils tested, this effect was not observed. The present paper shows that this effect must be expected in instruments for which count rate falls as density increases.

Belcher et al. (1), Carey and Reynolds (2), Kuranz (10), Carlton (3), Lauchaud (11), and Kuhn (9) reported that roughness of the surface beneath the instrument may affect the reading. This cause of error is discussed here.

Much experimental work has been done with gamma-ray backscatter instruments. However, an understanding of the factors which may affect the reading must come from a fundamental knowledge of all the processes which gamma radiation may undergo in the soil. This paper describes these processes and then relates them to the behavior of backscatter density gages.

## NOTATIONS

- a = distance from source to detector;
- b = constant equal to  $R_p/I$ ;
- d = effectively infinite depth;
- h = height of legs on apparatus;
- r = ratio of count on specimen to count on standard;
- p = probability of a photon remaining uncollided;
- t = time interval between calibration and use of instrument;
- x = distance;
- A = atomic weight of element;
- $E_0$  = energy of photon before collision, mev;

$E_i$  = energy of photon after collision, mev;  
 $F_i$  = mass fraction of  $i^{\text{th}}$  element in material,

$$\sum_{i=1}^{i=n} F_i = 1$$

$I$  = source intensity, photons/sec;  
 $I_c$  = source intensity at time of calibration;  
 $N$  = number of pulses detected in  $T$  sec;  
 $N_A$  = Avogadro number,  $0.6 \times 10^{24}$ /mole;  
 $R$  = net count rate;  
 $R_b$  = count rate due to background;  
 $R_p$  = net count rate when density is zero;  
 $R_s$  = count rate due to scattered photons;  
 $R_T$  = total count rate;  
 $S$  = sensitivity  $\equiv R'/R$ ;  
 $T$  = time interval for detecting  $N$  pulses, sec;  
 $Z$  = atomic number of an element;  
 $\Sigma$  = macroscopic reaction cross-section,  $\text{cm}^{-1}$ ;  
 $\sigma$  = standard error;  
 $\rho$  = density;  
 $\lambda$  = decay constant of source;  
 $\xi$  = Compton scattering cross-section per electron;  
 $\delta$  = reaction cross-section per atom;  
 $\theta$  = angle of scatter of photon.

## PHYSICAL PROCESSES

### Sources of Gamma Energy

An element which has been bombarded with elementary particles, so that the atomic nuclei possess excess energy, is unstable. The nuclei will return to a stable condition and in so doing may emit energy. This energy, which appears as particles called photons, is known as gamma energy and the isotope of an element emitting such energy is called a gamma-emitting isotope.

If a source of radiation is placed near a detector for  $T$  sec and  $N$  photons are counted in this time to give a count rate  $R = N/T$ , then  $N$  has a standard error of  $(N)^{1/2}$  due to the fundamental randomness of the radioactive decay process (4):

$$R = N/T \pm (N)^{1/2}/T \quad (1)$$

This relation is used later.

### Nuclear Cross-Sections

If a beam of energy photons penetrates a material, the photons may collide with the particles constituting that material. The probability that any one photon remains uncollided in distance  $x$  is

$$p = e^{-\Sigma x} \quad (2)$$

where  $\Sigma$ , the mean number of collisions per unit length for a beam of unit cross-section, is known as the macroscopic collision cross-section and is a measure of the probability that a collision will occur.

The probability that a particular type of colliding reaction will occur between a photon and any atom (i.e., the cross-section per atom for the reaction) is usually known from fundamental considerations. The cross-section per atom is related to the macroscopic cross-section in the following way: cross-section per cubic centimeter  $\text{cm} = \text{cross-section per atom} \times \text{number of atoms per cubic centimeter}$ . By Avogadro's law the number of atoms per cubic centimeter of an element is  $N_A \rho / A$ , where  $N_A$  is Avogadro number,  $\rho$  is density and  $A$  is atomic weight of the element. Therefore,

$$\Sigma = N_A \rho \delta / A \quad (3)$$

where  $\delta$  is the cross-section per atom.

When a beam of gamma photons enters a mass of soil, many reactions may occur between the photons and the atoms in the soil, but the only reactions of significance in this technique are Compton scattering and photoelectric absorption.

### Compton Scattering

Compton scattering is the scatter of a photon by an orbital electron. In this process, the binding energy of the electron to the nucleus has no effect. The cross-section per electron is given by the Klein-Nishina formula (4) and is dependent only on the incident photon energy. If  $\xi$  is this cross-section per electron, the cross-section per atom is  $Z\xi$  and from Eq. 3 the macroscopic cross-section  $\Sigma = N_A \rho Z\xi / A$ .

If the material is composed of  $n$  elements, the mass fraction of each being  $F_i$ , then the mass of each element per cubic centimeter is  $F_i \rho$  and the macroscopic cross-section is given by

$$\Sigma = \sum_{i=1}^n N_A \rho F_i Z_i \xi / A_i = N_A \rho \xi \sum_{i=1}^n F_i Z_i / A_i \quad (4)$$

At each scatter a photon loses energy. If  $E_0$  is the incident energy, and  $\theta$  is the angle of scatter, the energy of the scattered photon  $E_1$  is given by (4):

$$E_1 = \frac{E_0}{1 + \frac{E_0}{0.511} (1 - \cos \theta)} \quad (5)$$

### Photoelectric Absorption

In photoelectric absorption processes, the photon is absorbed by collision with an orbital electron tightly bound to the nucleus. The cross-section per atom is given approximately (14) by  $\delta = 1.25 \times 10^{-9} Z^5 E_0^{-7/2}$ . Therefore,  $\Sigma = k N_A \rho Z^5 / A$ , where  $k =$

$1.25 \times 10^{-9} E_0^{-7/2}$ . For a material comprising  $n$  elements,  $\Sigma = k N_A \rho \sum_{i=1}^n Z_i^5 F_i / A_i$ .

It should be noted that the quantity  $Z/A$  is very nearly  $1/2$  for all elements except hydrogen, for which it is almost 1. However, the mass of hydrogen per unit volume in soil is small because hydrogen is very light. Preiss and Newman (17) calculated

the quantities  $\sum_{i=1}^n F_i Z_i^5 / A_i$  and  $\sum_{i=1}^n F_i Z_i / A_i$  for a wide range of materials and showed

that the former varies from one material to another but the latter varies hardly at all. Therefore, absorption processes depend strongly on the elemental constitution of the

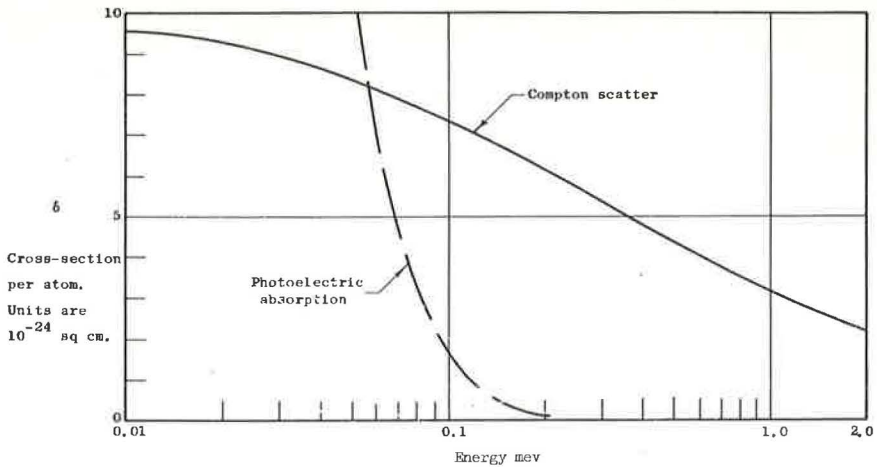


Figure 1. Photoelectric absorption and Compton scattering cross-sections per average atom of soil or concrete ( $Z = 15$ ,  $A = 31$ ) as a function of incident photon energy (from Grodstein, 1957).

material and scattering does not. It is apparent that any technique devised to measure the density of soils over a large range of soil types should be based on Compton scattering processes, with the influence of the photoelectric absorption reaction reduced to a minimum or entirely eliminated.

None of these processes depends on interatomic, crystalline or other forces. Although, in general, these forces may influence energy quanta, the effect at this range of energy is negligible. Gamma density methods measure the number of atoms per unit volume without regard to chemical binding forces and effects and, therefore, are insensitive to the structure of the material. For this reason, experimental results obtained on concretes are applicable to soils and vice versa.

Figure 1 shows the cross-sections for photoelectric absorption and Compton scattering as functions of photon energy. It is seen that between 0.1 and 2 MeV, Compton scattering is the only effective process. If, therefore, an apparatus can be made so that the photon energies are always in this range, the effect of chemical composition will be very small. It is shown in the following sections that such a solution is achievable when the detector "sees" the soil near the source.

#### CALIBRATION CURVES AND SOURCE-DETECTOR GEOMETRY

The general shape of the calibration curve for a backscatter density gage is shown in Figure 2. At zero density, no photons are scattered back to the detector, and the count rate  $R = 0$ .

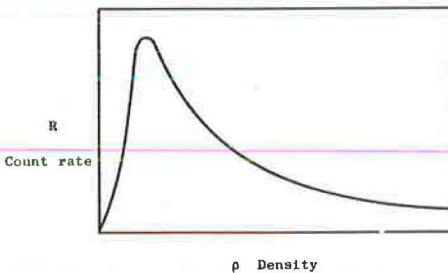


Figure 2. Calibration curve for backscatter density gage.

As the density of the material increases, two opposing processes occur. Although more photons are scattered towards the detector, photons directed towards the detector are again scattered and move away from it. At low densities, the number of scatters experienced by a detected photon is low, perhaps only one scatter. An increase in density in this range causes an increase in the count rate as the number of once- or twice-scattered detected photons increases. On the rising portion of the curve, the photons will have lost little energy.

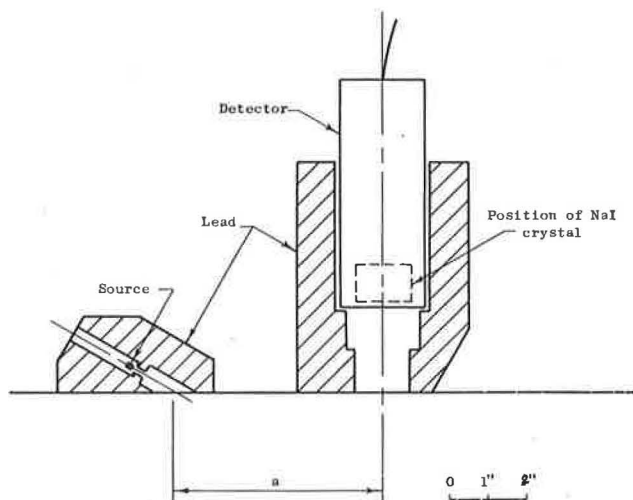


Figure 3. Source and detector arrangement for obtaining results with different geometries.

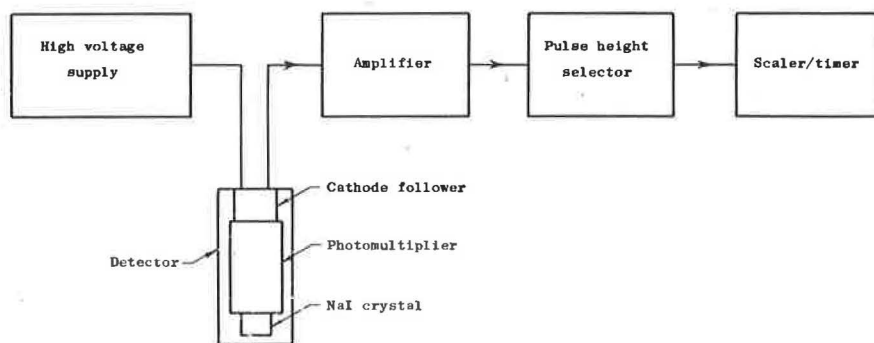


Figure 4. Block diagram of detection system.

At some density, the multi-scatter process begins to predominate; as few once- or twice-scattered photons survive to detection, the curve falls. As density increases further, the photons scatter more until their energy is reduced to that region in which photoelectric absorption probability is high. Thus, as  $\rho \rightarrow \infty$ ,  $R \rightarrow 0$ .

This hypothesis was tested experimentally using a scintillation counter with the apparatus shown in Figure 3. The source shield, which provided a collimated beam of photons, could be placed at any distance from the detector shield. The latter insured that the detector "saw" radiation only in a restricted volume.

Scintillation counters have the very useful property that the height or voltage of a pulse due to a detected gamma photon is proportional to the energy lost by that photon in the scintillator. By electronic sorting and counting of the pulses, the energies of photons being detected can be determined.

The detector (Fig. 4) consisted of a sodium iodide (NaI) scintillating crystal,  $1\frac{1}{2}$  in. in diameter and 1 in. thick, coupled by silicone grease to a photomultiplier. From the photomultiplier, the pulses were passed to a cathode follower, linear amplifier and then a pulse height selector, which passed only these pulses of amplitude (energy) falling within a preselected range. From the pulse height selector, the pulses passed to a scaler-timer unit for determining the count rate. By taking a series of counts over different ranges of pulse height, the pulse height distribution was obtained.

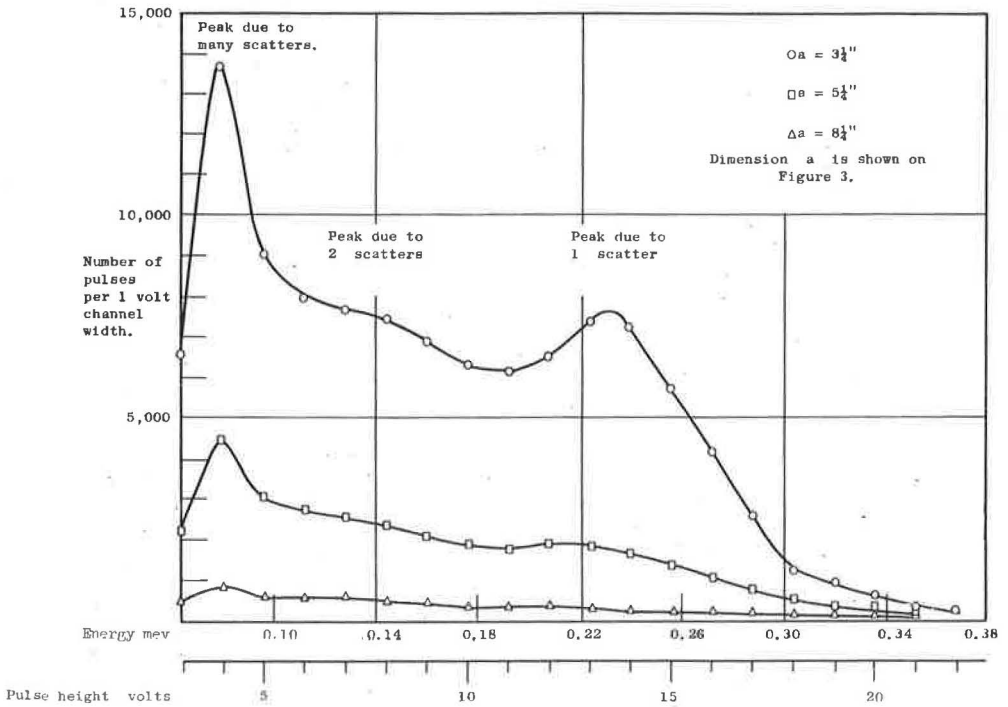


Figure 5. Pulse height distributions obtained on concrete block of density of 156 pcf using Cs-137, with various distances between source and detector.

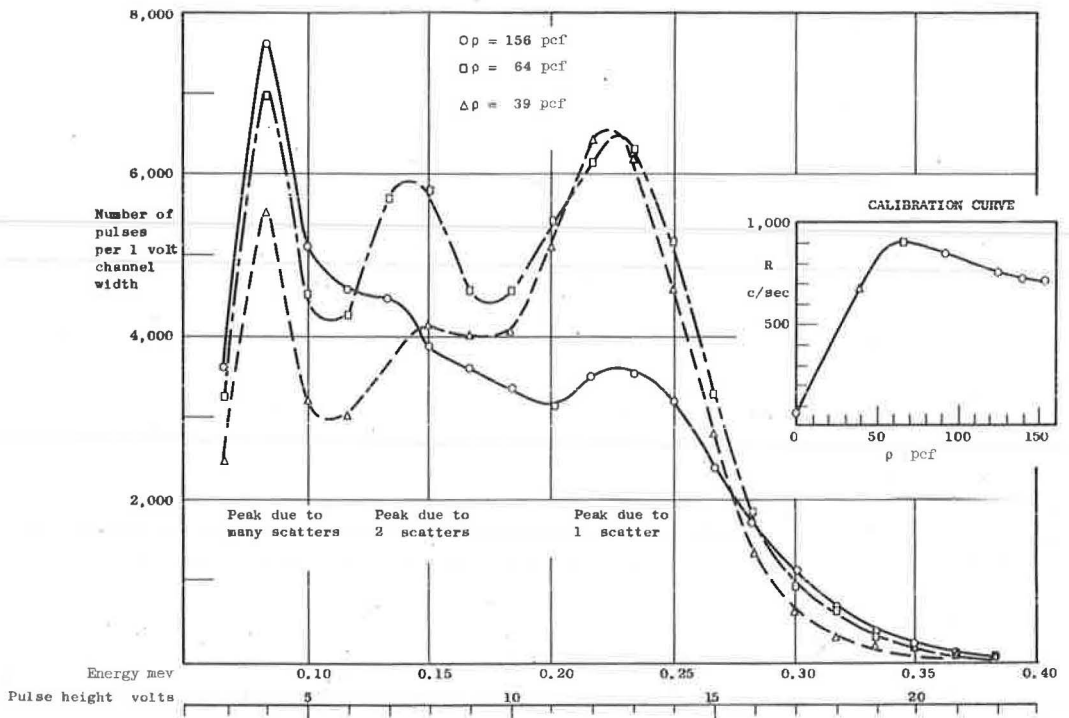


Figure 6. Calibration curve and pulse height distributions for a particular geometry (dimension  $a = 4\frac{1}{4}$  in.) on blocks of various densities.

Figure 5 shows the pulse height distributions obtained on a concrete block with a density of 156 pcf using a source of cesium 137 (source energy of 0.662 mev) with various distances from source to detector. As the distance from source to detector was increased, the relative intensity of high- to low-energy pulses decreased; i.e., the radiation became more times scattered.

The source energy was 0.662 mev, and the energy after scattering through 120 deg was calculated from Eq. 5 to be 0.224 mev. Therefore, the peak at that energy was due to the once-scattered photons. The peak at about 0.13 mev, small in Figure 5 but much larger in Figure 6, was due to twice-scattered photons. It has been observed (6, 7) that in a system such as this where the photons scatter through a given angle, by one, two or many scatters, the twice-scattered photons give a peak in the spectrum. The energy of twice-scattered photons was calculated as a function of scattering angle; for a Cs-137 source and a total angle of scatter of 120 deg, photons which suffered an initial large-angle scatter had final energy near 0.13 mev, giving the peak at that energy. At energies below 0.13 mev were photons which had scattered many times. If the concrete were a pure Compton scatterer, showing no absorption, the spectrum would reach infinity asymptotically as  $E \rightarrow 0$ , but because photoelectric absorption eliminated the lowest energy photons a peak was obtained. Hayward and Hubbell (7), Preiss (15) and others have shown that the position of the highest energy peak is dependent on the energy of the source, but the position of the intermediate energy peak is little affected and the position of the lowest peak is not affected.

Figure 6 shows pulse height distributions taken at three densities at a given geometry, together with the calibration curve at that geometry. At a density of 39 pcf, the number of once-scattered photons at 0.224 mev was relatively great and the calibration curve was rising. At 64 pcf, the relative number of twice- and more-times-scattered photons had increased and the calibration curve was at its peak. At 156 pcf, the number of once- and twice-scattered photons was reduced, most of the count rate was due to much scattered photons, and the calibration curve was falling.

If, therefore, the apparatus is arranged so that predominantly once- or twice-scattered photons are detected, the calibration curve will rise with density over the entire practical range. If, in addition, the detector is designed so as not to detect photons of energy less than 0.1 mev, the effect of photoelectric absorption and, therefore, of chemical composition will be minimized.

If the shield geometry is such that the calibration curve is a falling function of energy, the radiation will be much scattered and almost all the photons will be below 0.1 mev. If a bare Geiger-Müller detector is then used, low-energy photons will be detected, the photoelectric absorption reaction will be significant and an effect of the chemical composition of the soil must be expected.

When the detector "sees" soil near the source, high- and low-energy photons will be detected. The detection of photons of energy less than 0.1 mev must be avoided by using either a scintillation counter with appropriate pulse height selector or a Geiger-Müller tube with iron filters. In the latter case, the iron will absorb most of the low-energy photons before they reach the detector, but most of the higher energy photons will penetrate the iron. This method of eliminating the effect of chemical composition on the reading is analogous to the use of a cadmium cover for the same purpose in a neutron-scattering water content gage (16).

## DESIGN OF BACKSCATTER GAGE

Based on the preceding principles, a backscatter gage was designed and calibrated.

### Source

The source energy should be in the range of 0.1 to 2 mev so that the photons are subject to Compton scattering only. Practical sources in that energy range are cesium 137 and cobalt 60 (1.25 mev). Preiss (15) showed that source energy has little effect on the calibration curve. Cs-137, being easier to shield than Co-60 and having a longer half-life, was chosen; 5 millicuries being used.



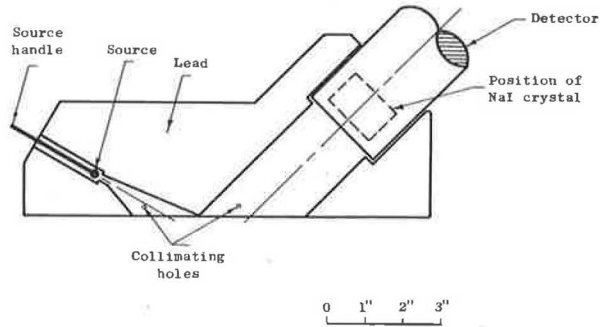


Figure 7. Backscatter gage.

### Shield

In order that the detected beam should include a high proportion of once- and twice-scattered photons so that the calibration curve will be a rising function of density and will be due to photons of energy greater than 0.1 mev over all practical ranges, the detector must "see" the material where the photons enter it. However, the detector itself must be separated from the source by several inches of lead to reduce the component of the count rate due to photons penetrating through the lead from source to detector. The geometry of the lead shield (Fig. 7) satisfied these requirements.

### Detector

The scintillation counter previously described was used with the pulse height selector set to pass only pulses exceeding 5 volts, which corresponded to 0.1 mev.

### CALIBRATION OF GAGE

Sixty concrete blocks, each 12 by 10 by 8 in., were made from a considerable range of concrete mixes. The mixes included mortars comprising ordinary portland cement

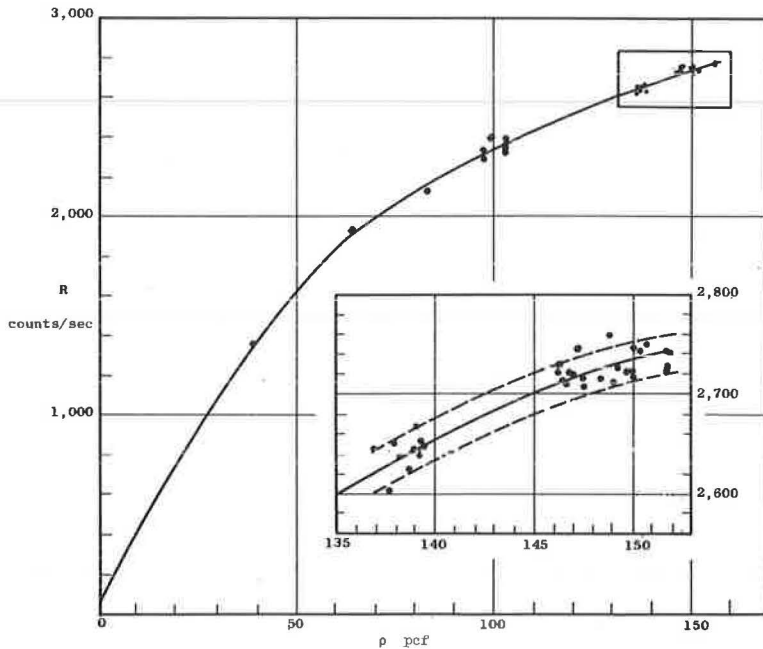


Figure 8. Calibration curve.



and a natural river sand, as well as concretes containing coarse aggregates including granite, river gravel, limestone, and expanded shale lightweight aggregate. The mix proportions were varied, the mixes having water-cement ratios ranging from 0.45 to 0.65 and aggregate-cement ratios ranging from 1.5 to 7.5. At densities below 100 pcf, larger factory-made lightweight blocks were used. Each block tested, therefore, had a chemical composition different from every other. It was shown earlier that the results obtained on the concrete blocks must be valid on soils.

The overall bulk density of each block was measured by weighing in air and water, and a count was taken with the apparatus. A curve of count rate against bulk density by weighing is shown in Figure 8, where the broken lines represent  $\pm 2$  standard errors due only to the statistics of nuclear counting; i.e., one point in 20 should, on the average, fall outside the broken lines.

The calibration curve is a curve of local density under the gage against overall density of the block, and this gave rise to apparent errors in the curve. Nevertheless, although the blocks covered a great variety of compositions, the scatter of the points was not much greater than would be expected from the statistical errors due to the randomness of nuclear decay.

#### ERROR DUE TO STATISTICS OF NUCLEAR COUNTING

The total count comprised radiation scattered off the concrete  $R_s$ , radiation penetrating the lead shield  $R_p$ , and background radiation due to cosmic and other sources  $R_b$ :  $RT = R_s + R_p + R_b$ . The background count  $R_b$  must always be subtracted to give the net count rate

$$R = R_s + R_p \quad (6)$$

For a given instrument,  $R_s$  is a function of density and  $R_p$  is a constant.

The expression relating density and count rate at a given source intensity  $I$  should be  $R_s = I F(\rho)$ . The exact form of  $F(\rho)$  is not relevant to this discussion. If  $R_p = b I$ , where  $b$  is a constant,

$$R = I F(\rho) + b I \quad (7)$$

If the count rate  $R$  is derived from  $N$  counts in  $T$  sec and if  $R_b \ll R$ , the standard deviation of  $R$ , from Eq. 1 is  $\sigma_R = R/(N)^{1/2}$ .

If the second derivation of  $R$  with respect to  $\rho$  is small,  $R(\rho)$  may be assumed to be linear over a small interval and  $\sigma_R/\sigma_\rho = dR(\rho)/d\rho \equiv R'(\rho)$ . Therefore,

$$\sigma_\rho = \sigma_R/R' = R/R' (N)^{1/2} \quad (8)$$

$$= [F(\rho) + b]/F'(\rho) (N)^{1/2} \quad (9)$$

$$= 1/S (N)^{1/2} \quad (10)$$

The factor  $R'/R$  is defined as the sensitivity of the apparatus, designated  $S$ . It is independent of the source intensity and is a function of  $\rho$ . To be used as a general measure for gamma backscatter apparatus, the value must be quoted at some standard density. If  $S$  is negative at this density, count rate is a falling function of density; if positive, it is a rising function. The accuracy obtainable may be completely specified by quoting both  $S$  and  $R$  at the standard density.

The factor  $(N)^{1/2}$  depends only on the number of counts taken.

The upper limit of  $S$  is reached as  $R_p \rightarrow 0$ , and is  $F'(\rho)/F(\rho)$ . The time  $T$  required to achieve a given standard error is given by

$$T = N/R = 1/S I F'(\rho) \sigma_\rho^2 \quad (11)$$

If the apparatus is calibrated when the source intensity is  $I$ , the source intensity any time  $t$  thereafter is given by  $I = I_0 e^{-\lambda t}$ . If, therefore, the relation between  $T$  and  $\sigma_\rho$  is determined at a given density at any time  $t = 0$ , the relation at time  $t$  will be  $T = e^{\lambda t} / S I_0 F'(\rho) \sigma_\rho^2$ .

As the source decays, the time required to achieve a given standard error increases. For Cs-137, this increase is about 2 percent per year. Unless the ratio of count on specimen to count on standard is used, the calibration curve must also be changed as time progresses.

If the count rate is changed by  $\Delta R$  due to surface roughness or another cause, the apparent error in density will be  $\Delta \rho = \Delta R / RS$ .

The value of sensitivity for the apparatus shown in Figure 7 was  $4.0 \times 10^{-3}$  cu ft/lb at a density of 100 pcf and gave a standard error of 0.3 pcf in 5 min. This error has since been reduced by better design of the apparatus geometry.

If, the ratio of count on the specimen to count on the standard, is used as the ordinate of the calibration curve, the sensitivity  $S$  just defined is given by  $S = r'/r$ , where  $r' \equiv dr/d\rho$ , and  $\sigma_\rho = 1/S \sqrt{1/N_1 + 1/N_2}$ .

Thus, using the ratio gives no change in sensitivity, but the calibration count  $N_1$  must be made several times larger than the specimen count  $N_2$  to give an error comparable with that of the count rate against density curve.

### REDUCING INFLUENCE OF SURFACE ROUGHNESS ON COUNT RATE

Roughness of a surface may be considered to raise the shield effectively above the "true" surface, reducing the path length between source and detector and, therefore, increasing the count rate. Since the base of the lead shield was plane, 4 in. wide by  $10\frac{3}{4}$  in. long, any protuberance over this area would have raised the shield and changed the count rate. Positioning three legs around the source and detector holes in the base is a logical method of reducing this effect (1, 2, 9).

The roughness of a surface compared with a plane surface may be defined by that height above the plane which gives the same count rate as the rough surface. Therefore, to reduce the effect of roughness, the apparatus should be used on legs of height  $h$  corresponding to a low value of the slope of the  $R$  vs  $h$  curve. This curve can easily be established experimentally.

Readings of count rate against height above a plane surface were taken using the apparatus of Figure 7 on two blocks of concrete, each 16 by 16 by 8 in. and with densities of 156 and 140 pcf. The curve of count rate against height above the surface is shown in Figure 9. Sensitivity at 140 pcf was calculated, assuming a linear calibration curve between 156 and 140 pcf; the curve of sensitivity against height is also shown in Figure 9.

For elimination of the effect of surface roughness on the reading, the legs should be of a height where the slope of the  $R$  vs  $h$  curve is a minimum. The peak at  $h = 0.3$  in. was probably too sharp to eliminate this effect satisfactorily; therefore, a height of 2.5 in. is more advisable for this shield. The statistical accuracy attainable in a given time at  $h = 2.5$  in. was,

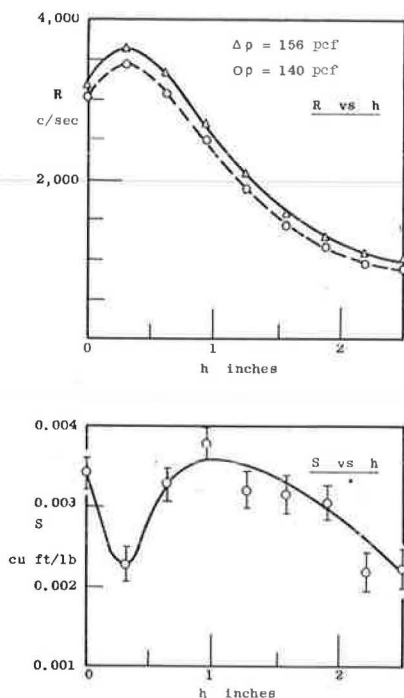


Figure 9. Count rate  $R$  and sensitivity  $S$  against leg height  $h$ .

however, reduced by changes in both count rate and sensitivity, so that, for this apparatus, reduction in the influence of surface roughness would have been attained by a sacrifice in time of count or accuracy.

### EFFECTIVELY INFINITE DEPTH

It is important to know to what depth the instrument will "see". Hayward and Hubbell (7) showed that the most-scattered photons penetrate furthest into a material, a result which may be expected. The effectively infinite depth is, therefore, determined by the low-energy photons shown in the distributions of Figures 5 and 6.

The probability that a photon survives distance  $d$  from the edge of the effectively infinite volume to the concrete surface, derived from Eqs. 2 and 3, is given by

$$p = e^{-N_A \rho \delta d/A} \quad (12)$$

where  $d$  is the effectively infinite depth.

For a given material cross-section  $\delta$  will be a function only of photon energy. The relevant photons are, however, all at the low-energy peak of Figures 5 and 6 so that  $\delta$  is constant. If the effectively infinite volume is defined by a constant value of probability  $p$ , then, because  $N_A$ ,  $A$  and  $\delta$  are constant,  $d \propto 1/\rho$ .

With every geometry of apparatus tested by the author,  $d$  was found to be 4 in. at a density of 140 pcf and to be inversely proportional to density. The effectively infinite depth was found to be independent of source energy or the distance between source and detector. The depth to which half the detected radiation penetrated did, however, increase from 1 to  $2\frac{1}{2}$  in. as the source and detector were moved from a separation distance of  $3\frac{1}{4}$  to  $7\frac{1}{4}$  in., at a density of 140 pcf.

### CONCLUSIONS

The error in density reading may be due to: (a) inaccurate calibration, (b) electronic drift, (c) chemistry of the soil, (d) surface roughness, or (e) statistics of nuclear counting. Although (a) and (b) are important, they were not discussed in this paper.

It has been shown here that the elemental constitution of the soil must affect the count rate when photons of energy less than 0.1 mev are detected. This occurs when the photons are much scattered and, at the same time, results in a calibration curve which falls as density increases. If only photons of energy exceeding 0.1 mev are detected, the soil-type effect becomes negligible. For these higher energy photons to be detected, the detector must "see" soil near the point at which radiation enters it. Once-, twice-, and more times-scattered photons are then detected. This geometry gives a calibration curve which rises with density. To prevent count of the photons of energy below 0.1 mev, a scintillation counter or filtered Geiger-Müller tube must be used.

The error in density reading due to the statistics of nuclear counting is given by equations whose useful application is in finding the best height of legs to reduce the effect of surface roughness. An example of the effect of leg height on the accuracy of a particular instrument is given. As was shown, the use of the slope of the calibration curve by itself as a figure of merit is meaningless; the ratio of slope to ordinate must be considered.

The effectively infinite depth was found to be 4 in. at a density of 140 pcf and was inversely proportional to density. This result was identical for all apparatus geometries and sources used.

Because it had previously been realized that the soil composition could affect the calibration curve, gages had to be calibrated for each soil. This was not a simple procedure. However, by designing the correct geometry of lead shield and by using the correct detector, the soil-type effect can be overcome.

## ACKNOWLEDGMENTS

The work reported here was done in the laboratories of the Nuclear Power Group, Department of Mechanical Engineering, Imperial College of Science and Technology, London. The author is grateful to P. J. Grant of the group and to A. L. L. Baker and K. Newman of the Department of Civil Engineering for encouragement and support.

## REFERENCES

1. Belcher, D. J., Cuykendall, T. R., and Sack, H. S. U. S. Civil Aero. Admin. Tech. Dev. Report No. 161, 1952.
2. Carey, W. N., Jr., and Reynolds, J. F. Some Refinements in Measurement of Surface Density by Gamma Ray Absorption. Highway Research Board Spec. Rept. 38, pp. 1-23, 1958.
3. Carlton, P. F. ASTM, STP 293, 1960.
4. Evans, R. D. The Atomic Nucleus. New York, McGraw-Hill, 1955.
5. Gnaedinger, J. P. ASTM, STP 293, 1960.
6. Hayward, E., and Hubbell, J. U. S. Nat. Bur. Std., Rept. 2264, 1953.
7. Hayward, E., and Hubbell, J. Jour. Appl. Phys., Vol. 25, No. 4, 1954.
8. Huet, J. Centre de Recherche Routieres, Brussels, Rept. 75/JH/1961, 1961.
9. Kuhn, S. H. Effects of Type of Material on Nuclear Density Measurements. Highway Research Record No. 66, pp. 1-14, 1965.
10. Kuranz, J. L. ASTM, STP 268, 1959.
11. Lauchaud, R. RILEM Bull. 13, 1961.
12. Mintzer, S. ASTM, STP 293, 1960.
13. Neville, O. K., and van Zelst, T. W. ASTM, STP 293, 1960.
14. Price, B. T., Horton, C. C., and Spinney, K. T. Radiation Shielding. Pergamon Press, 1957.
15. Preiss, K. Thesis, Univ. of London, 1964.
16. Preiss, K., and Grant, P. J. Jour. Sci. Instr. (London), Vol. 41, p. 548, Sept. 1964.
17. Preiss, K., and Newman, K. 4th Int. Conf. on Non-Destructive Testing. London, Butterworths, 1963.